

The Membrane Affinities of the Aliphatic Amino Acid Side Chains in an α -Helical Context Are Independent of Membrane Immersion Depth[†]

Charles J. Russell,[‡] Thorgeir Elís Thorgeirsson,[§] and Yeon-Kyun Shin*

Department of Chemistry, University of California, Berkeley, California 94720

Received May 19, 1998; Revised Manuscript Received September 3, 1998

ABSTRACT: Understanding, predicting, and designing the binding of peptides and proteins to bilayers require quantifying the intrinsic propensities of individual amino acid residues to bind membranes as a function of structural context and bilayer depth. A host–guest study was performed using the peptide host named helix5 in order to determine the membrane affinities of the aliphatic side chains both in an α -helical context and as a function of bilayer depth. Use of the α -helical host with a constrained geometry allowed the placement of guest sites at three different depths in bilayers and minimized secondary structural changes due to guest substitutions. Circular dichroism and electron paramagnetic resonance (EPR) were used to characterize the aqueous and bilayer-bound structures of the peptide variants. EPR was also used to measure the bilayer–water partition constants of the peptide variants, and the $\Delta\Delta G_{tr}$ values (relative to Gly) of the aliphatic amino acid side chains were subsequently calculated. Surprisingly, the $\Delta\Delta G_{tr}$ values did not significantly vary as a function of the guest site depth in bilayers. In addition, the $\Delta\Delta G_{tr}$ values determined in an α -helical context are reduced to approximately two-thirds of $\Delta\Delta G_{tr}$ values determined in other studies for the bilayer–water and octanol–water partitioning of amino acid side chains in extended and unstructured hosts. Both the relative reduction in $\Delta\Delta G_{tr}$ values in the context of an α -helical host and the invariance of $\Delta\Delta G_{tr}$ values with respect to bilayer depth are consistent with the membrane affinities of the aliphatic residues being largely determined by the classical hydrophobic effect.

Protein–lipid interactions are fundamental determinants of the structures and functions of many proteins. For example, membrane protein folding involves a series of steps in which proteins first insert into membranes and then fold into their native tertiary structures within membranes (2–4). Protein–lipid interactions also play critical roles in the mechanisms of membrane fusion in biological processes such as neurotransmission (5, 6), viral infection (7–9), and egg fertilization (10, 11). In addition, protein–lipid interactions are involved in the activity of antimicrobial peptides (12–14), the translocation of toxins (15), and the targeting of signal sequences (16–19). However, it has been difficult to analyze the protein–lipid interactions of many specific biochemical systems due to experimental difficulties. An alternative is first to quantify the energetic contributions which determine protein structure and bilayer–water partitioning using simple, model peptides. Such minimalistic studies then may lead to the successful understanding, prediction, and design of specific biochemical systems of interest. The purpose of this work was to determine the intrinsic propensities of the aliphatic amino acid side chains to bind membranes (also known as the membrane affinities or $\Delta\Delta G_{tr}$ values¹) in the context of an α -helical peptide and

to assess whether these propensities vary as a function of the depth of the side chains in membranes.

A long-held view regarding the transfer of peptides from water to membranes is that the transfer can be modeled simply as the hydrophobic removal of peptides from bulk water into bulk nonpolar phase (20). In fact, nearly all of the large number of hydrophobic indices for amino acids (for a listing of 82 indices, see ref 21) are based on physical properties of small peptides and side chain analogues and on the distribution of amino acids in proteins. However, phospholipid bilayers are chemically heterogeneous (22–24), and the polarity of any given amino acid residue's environment within a bilayer may not necessarily be equivalent to bulk nonpolar solvent due to differences in

[†] Supported by NIH Grant GM51290. Y.-K.S. is a 1995 Searle Scholar.

* To whom correspondence should be addressed.

[‡] Present address: BMBCB, Howard Hughes Medical Institute, Northwestern University, 2153 North Campus Dr., Evanston, IL 60208.

[§] Present address: Decode Genetics, Lyngbals 1, 110 Reykjavik, Iceland.

¹ Abbreviations: Ac-, acetylated amino terminus; CD, circular dichroism; DCC, N,N'-dicyclohexylcarbodiimide; DOPC, dioleoylphosphatidylcholine; EDDA, ethylenediamine-N,N'-diacetic acid; EPR, electron paramagnetic resonance; Fmoc, 9-fluorenylmethoxycarbonyl; GuCl, guanidine chloride; KCl, potassium chloride; LUV, large unilamellar vesicle; MOPS, 3-(N-morpholino)propanesulfonic acid; MTSSL, S-(1-oxy-2,2,5,5-tetramethylpyrroline-3-methyl)methanethiosulfonate spin-label; NH₄OAc, ammonium acetate; NMP, 1-methyl-2-pyrrolidinone; NMR, nuclear magnetic resonance; P_b , concentration of peptide bound to bilayers; P_f , concentration of peptide free in aqueous solution; pCoxIV, presequence of yeast cytochrome c oxidase subunit IV; POPC, 1-palmitoyl-2-oleoylphosphatidylcholine; POPG, 1-palmitoyl-2-oleoylphosphatidylglycerol; HPLC, high-performance liquid chromatography; SUV, small unilamellar vesicle; TFA, trifluoroacetic acid; TFE, 2,2,2-trifluoroethanol; $\Delta\Delta G_{tr}$, difference in standard-state Gibbs transfer free energies due to nonelectrostatic contributions; $[\theta]_{222}$, mean residue ellipticity at 222 nm; $[\theta]_H$, mean residue ellipticity at 222 nm for a completely α -helical peptide; -NH₂, amidated carboxy terminus.

immersion depth (25). In addition to the hydrophobic effect, other thermodynamic forces such as electrostatic interactions, peptide immobilization, peptide conformational changes, "bilayer effects", and van der Waals dispersion forces can participate in the water-membrane partitioning of peptides (26-29).

To investigate the nonelectrostatic forces governing the partitioning of peptides between water and membranes, the bilayer-water transfer free energies (ΔG_{tr} values) of a variety of short peptides have been measured. The results from quantitative studies on the partitioning of non- α -helical peptides are consistent with the hydrophobic effect being the main (although not necessarily exclusive) driving force behind the bilayer insertion of such peptides (27, 29, 30). Experimentally determined membrane affinities ($\Delta\Delta G_{tr}$ values) of individual amino acid side chains, measured in host-guest systems employing unstructured and extended hosts, are also consistent with the hydrophobic effect being the driving force behind bilayer insertion (27, 31, 32). However, there is disagreement as to whether the guest amino acid side chains experience the full magnitude of the classical hydrophobic effect (31) or only approximately half (32) upon removal from water and insertion into bilayers. One possible explanation for the conflicting results is that the $\Delta\Delta G_{tr}$ values of amino acid side chains vary as a function of the bilayer depth of the guest sites due to polarity gradients in membranes. The host-guest study performed by Thorgeirsson et al. (31) used an extended/unordered 25-residue host with a guest site located in the acyl chain region of bilayers in the membrane-bound state, whereas the host-guest study performed by Wimley and White (32) used an unstructured pentapeptide host with a guest site located in the headgroup region of bilayers. However, $\Delta\Delta G_{tr}$ values have not yet been experimentally determined either as a function of bilayer depth or in an α -helical context.

To determine the $\Delta\Delta G_{tr}$ values of the aliphatic side chains both in an α -helical context and as a function of membrane-bound depth, we performed a host-guest study using the α -helical peptide host named helix5 (33). Use of the geometrically constrained host minimized structural changes due to guest substitutions and allowed the $\Delta\Delta G_{tr}$ values to be determined for different regions of bilayers. Fifteen peptide variants of helix5 were synthesized with Gly, Ala, Val, Ile, and Leu residues substituted separately at each of three guest sites. The guest sites were located in the acyl chain region, the interface of the acyl chain and headgroup regions, and the headgroup region of bilayers in the bilayer-bound states. Circular dichroism (CD) and electron paramagnetic resonance (EPR) experiments were used to characterize the aqueous and bilayer-bound secondary structures of the peptide variants. EPR was also used to measure the partitioning of the peptides between aqueous solution and bilayers. From the partitioning data, $\Delta\Delta G_{tr}$ values (relative to Gly) for the aliphatic amino acid side chains were calculated. The $\Delta\Delta G_{tr}$ values do not appear to vary as a function of the bilayer-bound depth of the guest site. Moreover, the $\Delta\Delta G_{tr}$ values for bilayer-water transfer in an α -helical context are reduced to about two-thirds of $\Delta\Delta G_{tr}$ values for both bilayer-water transfer (31) and octanol-water transfer (34, 35) using peptides with guest side chains nearly fully exposed to solvent. Both results are consistent with the membrane affinities of the aliphatic side chains

being largely determined by the classical hydrophobic effect, which is manifested by the removal of nonpolar surface area from bulk water and is independent of the bilayer-bound depths of the aliphatic guest side chains.

MATERIALS AND METHODS

Materials. Rink amide MBHA resin and N- α -Fmoc-amino acid derivatives were purchased from Calbiochem-Novabiochem Corp. 4-Hydroxy-TEMPO and *S*-(1-oxy-2,2,5,5-tetramethylpyrroline-3-methyl)methanethiosulfonate spin-label (MTSSL) were obtained from Aldrich Chemical Co. and Toronto Research Chemical (Ontario, Canada), respectively. 1-Palmitoyl-2-oleoylphosphatidylcholine (POPC) and 1-palmitoyl-2-oleoylphosphatidylglycerol (POPG) were obtained from Avanti Polar Lipids (Alabaster, AL). Ni-EDDA was prepared from EDDA and Ni(OH)₂ according to a method developed by Christian Altenbach (unpublished).

Peptide Synthesis and Purification. The amino acid² sequence of the peptide host, helix5, is Ac-NELKKKLELCKAKWLEAKKKLEALK-NH₂. The underlined residues at positions 7, 9, and 12 in the amino acid sequence correspond to the guest sites. The peptide helix5 was synthesized previously (33). The peptide variants of helix5 were synthesized by solid-phase peptide synthesis using N- α -Fmoc-amino acid derivatives and Rink amide resin. For all of the peptides, the 13 carboxy-terminal residues are identical and were synthesized by automated synthesis on an Applied Biosystems 431 synthesizer. The resulting precursor peptide attached to the resin was then split into smaller batches, and the remaining residues were coupled in parallel by hand using a 2 × 5 array of reaction vessels purchased from SynPep Corp. (Dublin, CA). The peptide helix5b has the same amino acid² sequence as helix5 except for Leu7Ala and Ala12Leu substitutions: Ac-NELKKKAELCKLKWLEAKKKLEALK-NH₂. Helix5b was synthesized entirely by automated synthesis. All of the peptides were amino-terminus-acetylated by reacting with a 5-fold molar excess of acetic anhydride for 1 h in the presence of a 5-fold molar excess of *N,N*-diisopropylethylamine (DIPEA). The peptides were cleaved from the resin and side chain deprotected by reacting with Reagent K for 3-6 h (36). Excess trifluoroacetic acid (TFA) was removed by rotary evaporation, and the peptides were subsequently precipitated in excess cold *tert*-butyl methyl ether. The peptides were washed by seven cycles of mixing in *tert*-butyl methyl ether, spinning the peptides into pellets, and decanting the ether. The peptides were then dried overnight in a vacuum desiccator. The peptides were purified to >95% purity by reversed-phase HPLC using a Vydac C₁₈ column and a water/acetonitrile (0.1% TFA) gradient. The identity and purity of each peptide were confirmed by electrospray-ionization mass spectrometry using a Hewlett-Packard Model 5989A mass spectrometer.

Spin-Labeling. Each of the purified peptide variants were spin-labeled at the cysteine at position 10 with *S*-(1-oxy-2,2,5,5-tetramethylpyrroline-3-methyl)methanethiosulfonate spin-label (MTSSL). The peptides were dissolved in mixtures of 5 mM potassium phosphate buffer (pH 7.0, 10

² The one-letter abbreviations for the amino acids are as follows: A = Ala, C = Cys, D = Asp, E = Glu, F = Phe, G = Gly, H = His, I = Ile, K = Lys, L = Leu, M = Met, N = Asn, P = Pro, Q = Gln, R = Arg, S = Ser, T = Thr, V = Val, W = Trp, and Y = Tyr.

mM KCl) and 250 μ L of acetonitrile. Appropriate volumes of 50 mM MTSSL in acetonitrile were added to the peptide solutions so that the concentrations of MTSSL were in 2-fold molar excess of the peptides. After allowing the spin-labeling reactions to proceed for at least 1 h, the spin-labeled peptides were purified by reversed-phase HPLC using a water/acetonitrile (0.1% TFA) gradient. Fractions containing the spin-labeled peptides were collected as single peaks, lyophilized, and stored dry at -20°C . The identity and purity of the spin-labeled peptides were confirmed by mass spectrometry.

Lipid Vesicle Preparation. Stock solutions of POPC and POPG in chloroform were mixed by volume to obtain the appropriate molar ratios of negatively charged phospholipids. Most of the chloroform was evaporated under a stream of nitrogen gas, and the lipid mixtures were lyophilized overnight to remove trace amounts of chloroform. The lipids were suspended at room temperature in either 5 mM potassium phosphate buffer (pH 7.0, 50 mM KCl) or 5 mM MOPS buffer (pH 7.0, 50 mM NH_4OAc) to yield a total lipid concentration of 75 mM. After 7 cycles of freezing and thawing, the lipid solutions were passed through 100 nm pore size polycarbonate membranes using an Avanti Mini-Extruder (Avanti Polar Lipids; Alabaster, AL) to prepare large unilamellar vesicles (LUVs). Small unilamellar vesicles (SUVs) were prepared by diluting lipid stock solutions (5 mM potassium phosphate buffer, pH 7.0, 50 mM KCl, 15 mol % POPG/POPC) to 30 mM and sonicating the lipid solutions for approximately 1 h. The resulting solutions were clear.

CD Spectroscopy. CD spectra of the spin-labeled peptides in aqueous solution and $[\theta]_{222}$ values in SUVs were recorded on Aviv Model 62 DS spectropolarimeters at 25°C . The spectra were measured at 1 nm intervals with a 1.5 nm bandwidth and a 15 s time constant. The $[\theta]_{222}$ values were measured at 1 s intervals for 60 s with a 1.5 nm bandwidth and a 1 s time constant. Spin-labeled peptide solutions were buffered with 5 mM potassium phosphate (pH 7.0, 50 mM KCl), and the SUV samples contained 15 mM lipid consisting of 15 mol % POPG/POPC. Peptide concentrations were determined by the absorbance at 280 nm in 6 M GuCl (37). The peptide concentrations in aqueous solution ranged from 60 to 90 μM , and the peptide concentrations in SUVs ranged from 30 to 45 μM . The final lipid concentrations in the samples containing SUVs were 15 mM, so the peptide:lipid ratios ranged from 1:333 to 1:500. All of the peptides in the samples containing SUVs were determined to be bound to SUVs by EPR spectral subtraction. The percent of peptide in an α -helical conformation was estimated by the equation:

$$\% \alpha\text{-helix} = \frac{[\theta]_{222}}{[\theta]_{\text{H}}} \times 100\% \quad (1)$$

where $[\theta]_{222}$ is the mean residue ellipticity at 222 nm in $\text{deg cm}^2 \text{dmol}^{-1}$ and $[\theta]_{\text{H}}$ is the predicted mean residue ellipticity at 222 nm for the completely α -helical peptide in $\text{deg cm}^2 \text{dmol}^{-1}$. The $[\theta]_{\text{H}}$ values were determined by trifluoroethanol (TFE) titration to account for aromatic side chain contributions to the far-ultraviolet CD (38).

EPR Power Saturation Measurements of Membrane-Bound Depths. The EPR collision gradient method developed by Altenbach et al. (39) was used to determine the bilayer-bound

depths of the spin-labels at position 10 in each of the peptide variants as described previously (33). The depth measurements required that all of the peptides were bound to the LUVs in each sample. To ensure that all the peptides were bound to LUVs, we prepared the peptide samples in 15 mol % negatively charged LUVs. Each of the peptides was dissolved in 5 mM MOPS buffer (pH 7.0, 50 mM NH_4OAc) with 75 mM of 15 mol % POPG in POPC, so that the final lipid concentration was 50 mM. A gas-permeable TPX capillary was used to allow saturation of the samples with air or $\text{N}_2(\text{g})$. EPR spectra were recorded at 0.101, 0.250, 0.400, 0.800, 1.27, 2.01, 4.00, 6.35, 10.1, 16.0, 25.3, and 40 mW of incident power in the presence of $\text{O}_2(\text{g})$, $\text{N}_2(\text{g})$, and $\text{N}_2(\text{g})/\text{Ni-EDDA}$. Ni-EDDA concentrations of 200 mM were used. The peak-to-peak amplitudes of the first-derivative $M_1 = 0$ lines were used to obtain saturation profiles. The power saturation profiles were fitted by a nonlinear least-squares algorithm to determine the $P_{1/2}$ values and subsequently $\Delta P_{1/2}$ values (39). The natural log of the ratio of $\Delta P_{1/2}$ values in the presence of water-soluble (e.g., Ni-EDDA) and membrane-soluble (e.g., O_2) fast-relaxing agents (Φ) is directly related to the difference in standard state chemical potentials of the reagents at any depth and is proportional to the bilayer-bound depth according to the expression (39):

$$\Phi = \ln \frac{\Delta P_{1/2}(\text{O}_2)}{\Delta P_{1/2}(\text{Ni-EDDA})} = S \cdot D + C \quad (2)$$

where S is the slope, D is the distance of the nitroxide from the lipid phosphate groups in angstroms, and C is the intercept. A calibration performed previously yielded a slope (S) of 0.27 \AA^{-1} and an intercept (C) of -1.16 (33). After determining the $\Delta P_{1/2}$ values, the distances from the nitroxide spin-labels to the lipid phosphates were calculated according to eq 2, and errors in the EPR-determined depths of the spin labels were determined by an analysis of the propagation of fitting errors.

EPR Measurements of Bilayer-Water Partitioning. EPR spectra were collected using a Bruker ESP300 EPR spectrometer (Bruker Instruments) equipped with a low-noise microwave amplifier (Mitech) and a loop-gap resonator (Medical Advances). The loop-gap resonator was inserted into a homemade quartz vacuum Dewar, and the temperatures of the samples were maintained at $25 \pm 1^{\circ}\text{C}$ by a Eurotherm V-VT 200 thermostat. A modulation amplitude of 0.5 G was used. Samples were prepared by mixing peptide and lipid solutions in a 1:2 ratio and letting the solutions equilibrate for at least 0.5 h before EPR measurements. The EPR-determined partition constants did not vary over time for samples measured periodically over 1 week. The final concentrations of bilayer-bound (P_b) and aqueous (P_i) peptide fractions in the lipid-containing samples were determined by EPR spectral subtraction. The total concentrations of peptides (between 80 and 230 μM) were determined by comparing their doubly integrated spectra to that for a 100 μM solution of the standard 4-hydroxy-TEMPO. Concentrations determined by this method are greater than 95% accurate. The final concentration of lipids in the samples was 50 mM, so the peptide:lipid ratios ranged from 1:217 to 1:625. The total concentrations of peptide were varied so that under any given sample condition (e.g., mol % of negatively charged lipid) the concentration of peptide bound

to bilayers (P_b) was between 50 and 60 μM . Therefore, the ratios of bilayer-bound peptide:lipid were approximately 1:900. The samples were buffered by 5 mM MOPS buffer (pH 7.0, 50 mM NH_4OAc).

Thermodynamics of Bilayer–Water Partitioning Equilibria. The concentrations of peptide bound to bilayers (P_b) and free in aqueous solution (P_f) were determined by EPR spectral subtraction. The incorporation of the peptides into membranes was analyzed using the partitioning model (29):

$$K_{\text{app}} = \frac{X_b}{X_f} = \frac{P_b C_w}{P_f C_L} \quad (3)$$

where K_{app} is the apparent partition constant in unitary units (20, 40), X_b is the mole fraction of bilayer-bound peptide, X_f is the mole fraction of aqueous peptide, C_w is the concentration of bulk water (55.5 M), and C_L is the lipid concentration.

To keep the $P_b:P_f$ ratios as close to unity as possible for spectroscopic accuracy, LUVs containing either 7 or 9 mol % of negatively charged lipids were used. The resulting $P_b:P_f$ ratios were between 0.2 and 1.7. The peptides used in the partitioning experiments had a net charge of +5, and the LUVs had a net negative charge. Therefore, it was necessary to consider the charge–charge contributions to membrane binding before determining the noncharged contribution to the differences in transfer free energies ($\Delta\Delta G_{\text{tr}}$). To negate differences in membrane surface potentials experienced by any two peptides which were compared to determine $\Delta\Delta G_{\text{tr}}$ values, the total concentrations of compared peptide samples were varied so that under the given sample condition (e.g., mol % of negatively charged lipid) the difference in concentrations of peptide bound to bilayers (P_b) was $<5 \mu\text{M}$. Even though two compared peptide samples had different partition constants due to different concentrations of peptide in aqueous solution, the two samples had approximately the same concentration of bilayer-bound peptide and, therefore, experienced approximately the same contribution of membrane binding due to charge–charge interactions. The nonelectrostatic contributions to the differences in bilayer–water transfer free energies ($\Delta\Delta G_{\text{tr}}$ values) were determined for each pair of peptides by eq 4:

$$\Delta\Delta G_{\text{tr}} = -RT \ln \left(\frac{K_{\text{app}2}}{K_{\text{app}1}} \right) - zF(\Psi^2 - \Psi^1) \quad (4)$$

$$\Delta\Delta G_{\text{tr}} = \Delta\Delta G_{\text{tot}} - \Delta\Delta G_{\text{el}} \quad (5)$$

where RT equals 0.592 kcal mol $^{-1}$ at 298.15 K, z is the formal charge on the peptide, F is Faraday's constant, Ψ is the surface potential (41), $\Delta\Delta G_{\text{tot}}$ is the total difference in standard-state Gibbs transfer free energies, and $\Delta\Delta G_{\text{el}}$ is the difference in standard-state Gibbs transfer free energies due to charge–charge interactions between peptides and lipids. The differences in Ψ values were small since for any two compared peptides the differences in P_b values were small ($<5 \mu\text{M}$) and the lipid and buffer solutions had the same composition. As a result, the differences in electrostatic contributions to bilayer binding ($\Delta\Delta G_{\text{el}} = zF\Delta\Psi$) for any given pair were <0.1 kcal mol $^{-1}$.

RESULTS

The α -Helical Host–Guest System. An ideal α -helical peptide host should have the following properties: (a)

maximum α -helicity in aqueous solution and in bilayers with minimal structural changes upon phase transfer, (b) monomeric structure both in aqueous solution and in bilayers to avoid energetic contributions due to oligomerization, (c) reversible binding to bilayers to allow quantitative measurements of water–membrane partitioning, and (d) guest sites completely buried in the bilayer in the bilayer-bound states. In addition, an ideal α -helical peptide host should not undergo changes in α -helicity due to guest substitutions. However, the α -helix propensities of amino acid residues vary significantly (42–44). Due to possible structural changes resulting from guest substitutions, the aqueous and bilayer-bound structures for each peptide variant should be characterized before relationships between $\Delta\Delta G_{\text{tr}}$ values and guest substitutions can be analyzed.

The 25-residue peptide host used in this study, helix5, was designed previously (33) and meets the aforementioned criteria relatively well. Analytical ultracentrifugation and CD experiments showed that helix5 is monomeric and approximately 81% α -helical in aqueous solution at 25 °C (5 mM potassium phosphate buffer, pH 7.0, 10 mM KCl). EPR power saturation experiments with a cysteine-scanning strategy showed that helix5 binds parallel to the surface of bilayers as an α -helix with a central helical axis located approximately 5 Å below the phosphate groups in the lipids (Figure 1a). Helix5 is an amphipathic peptide with a nonpolar face at the “a” and “d” positions, a nonpolar–polar interface at the “e” and “g” positions, and a polar face at the “b”, “c”, and “f” positions. The EPR-determined depths and the distribution of nonpolar and charged residues in helix5 (Figure 1) are consistent with the lysine residues at the nonpolar–polar interface “snorkeling” so that the central axis of the α -helix is positioned in the acyl chain region of the phospholipid bilayers and the polar face of the α -helix is buried in the headgroup region (45). The bilayer-bound topology of helix5 allows guest sites to be located in the acyl chain (position 7), the interface between acyl chain and headgroup (position 9), and headgroup (position 12) regions of the bilayer in the bilayer-bound states (Figure 1b). EPR spectroscopy also showed that helix5 partitions between aqueous solution and LUVs with a ratio of bilayer-bound (P_b) to aqueous (P_f) peptide near unity under certain conditions.

Peptide Structures as a Function of Guest Substitutions. Analytical ultracentrifugation, CD, and EPR experiments show that the peptide host helix5 has a monomeric structure in aqueous solution and when bound to bilayers (33). Moreover, the EPR spectra for all of the peptides with guest substitutions are characteristic of fast-motional EPR spectra for short, monomeric α -helical peptides and have line shapes independent of concentration between 50 and 150 μM . The CD spectra of the peptide variants in aqueous solution have minima at approximately 208 and 222 nm and are characteristic of spectra undergoing a two-state helix–coil transition with an isodichroic point near 203 nm (data not shown). The $[\theta]_{222}$ values and % α -helix values for the peptides in aqueous solution are listed in Table 1. The % α -helix values fall into two classes: the peptides with Gly residues as guests are $52 \pm 5\%$ α -helical, and the peptides with Ala, Val, Ile, and Leu residues as guests are $74 \pm 8\%$ α -helical. The significantly lower % α -helix values for the peptides with Gly residues as guests are consistent with Gly having a low

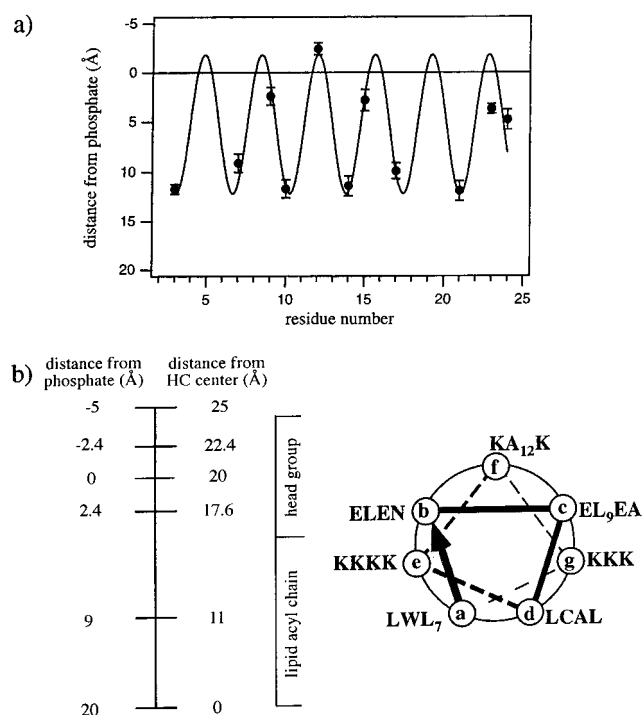


FIGURE 1: (a) Bilayer-bound structure of helix5 (33). The solid circles are the EPR-determined distances from lipid phosphate groups to the spin-labels scanned through the sequence of helix5. The positive distances are directed toward the center of the membrane, and the negative distance is directed toward the aqueous phase. The data fit well to a model (solid sine wave) in which helix5 is bound to bilayers parallel to the surface as an α -helix of 3.6 residues/turn with the center of the helix positioned at a depth of 5 Å from the phosphate groups. The guest sites were placed at positions 7, 9, and 12 in the sequence which correspond to spin-labeled distances from the lipid phosphate groups of 9.1 ± 0.9 , 2.4 ± 0.9 , and -2.4 ± 0.6 Å, respectively. (b) Sequence of the peptide host, helix5, projected on a heptad repeat. The guest sites at positions 7, 9, and 12 reside in the acyl chain, acyl chain/headgroup interface, and headgroup regions of the bilayer, respectively. The nitroxide spin-label MTSSL was covalently attached to the cysteine at position 10 in all of the peptide variants.

α -helix propensity (42–44) and may arise from partial α -helix uncoiling near the guest site. The peptides with Ala, Val, Ile, and Leu residues as guests have α -helix contents of approximately 74%, with no trend of higher or lower α -helix propensities between the guest residues.

The α -helix contents of the peptides with Ala, Val, Ile, and Leu as guests are also approximately 75% when bound to SUVs (Table 1). EPR experiments showed that all of the peptides were bound to SUVs in the SUV-containing samples used for CD experiments. The % α -helix values for the peptides with Gly substitutions at positions 7, 9, and 12 are 67, 59, and 73%, respectively. The α -helix contents of the SUV-bound peptide variants with Ala, Val, Ile, and Leu as guests at all three guest sites are very similar, have an average value of $75 \pm 5\%$, and do not significantly differ from their α -helix contents in aqueous solution ($74 \pm 8\%$). Since CD is only sensitive to global secondary structure, it is still possible that these peptides undergo minor secondary structure changes due to guest substitutions and/or bilayer–water transfer.

EPR power saturation experiments showed no changes in the bilayer-bound depths of the spin-labeled peptide variants due to guest substitutions. Each peptide variant was spin-

labeled with MTSSL at the cysteine at position 10 in the sequence. EPR power saturation profiles were measured for each of the peptide variants in the presence of $O_2(g)$, $N_2(g)$, and $Ni \cdot EDDA/N_2(g)$. The distances from the nitroxide spin-labels to the lipid phosphates were calculated according to eq 2 and are included in Table 1. The bilayer-bound depths of the spin-labels at position 10 do not appear to vary as a function of guest residue substitution, ranging between 11.0 and 12.3 Å, which is within the experimental uncertainties of the measurements. Given the uncertainties in the EPR depth measurements, it is possible, albeit unlikely, that the host α -helix reorients its helical axis with respect to the bilayer surface as a result of the guest substitutions. Based on a geometric analysis of the bilayer-bound peptide modeled as a heptad repeat (Figure 1b) and the experimental values for the nitroxides at position 10 in the peptides (Table 1), the α -helix could rotate up to 72° with the spin-label at position 10 still located between 11.0 and 12.4 Å. However, such rotations of the α -helix would also cause the positively charged lysine side chains to move up to 5.4 Å deeper into the acyl chain region of the bilayer (see Figure 1b) which would be extremely unfavorable energetically (25). Moreover, the EPR-determined depths of the MTSSL spin-labels substituted throughout the peptide host (Figure 1a) are inconsistent with depths which would result from angular reorientation of the α -helix in response to the spin-label, which has a hydrophobicity comparable to that of the leucine side chain (31).

Given the periodicity of charged and hydrophobic residues in the peptide host (Figure 1b), the α -helix content of approximately 75% in aqueous solution and in SUVs, and the constant membrane depth of the spin-labeled residues at position 10, it is unlikely that the Ala, Val, Ile, and Leu guest substitutions cause major structural changes in the bilayer-bound states. Moreover, with the spin-labeled residues at position 10 located in the acyl chain region of the bilayers 11.7 ± 0.7 Å from the lipid phosphates, disruption of the α -helical structure near the guest sites could result in the burial of charged groups in the acyl chain region of the bilayers, which is energetically costly. A combination of the CD and EPR power saturation results and energetic considerations strongly suggests that the bilayer-bound structures of the peptide variants with Ala, Val, Ile, and Leu as guests do not significantly change as a function of guest substitutions.

Membrane Affinities ($\Delta\Delta G_{tr}$ Values) of Aliphatic Side Chains in an α -Helical Context. EPR spectra were collected for each of the peptide variants in the presence and absence of LUVs. For example, Figure 2 shows the EPR spectra for helix5, which contains Ala at position 12 and Leu at positions 7 and 9. EPR spectral subtraction was used to determine the concentrations of bilayer-bound (P_b) and aqueous (P_f) peptide in the lipid-containing samples (Figure 2). Once the $P_b:P_f$ ratios were determined for the peptide samples, the membrane affinities ($\Delta\Delta G_{tr}$ values) for sets of guest side chains under the same sample conditions (same lipid composition, buffer, and P_b values) were calculated according to eq 4. Determining $\Delta\Delta G_{tr}$ values for guests under the same conditions ensured that the compared peptides experienced the same membrane surface electrostatic potentials, which could then be subtracted out to yield $\Delta\Delta G_{tr}$ values which are independent of electrostatic contributions to bilayer

Table 1

guest ^a	guest bilayer location ^b	$\Delta\Delta G_{tr}$ (kcal mol ⁻¹) ^c	membrane depth at position 10 ^d	$[\theta]_{222}$ aqueous ^e	% α -helix aqueous ^f	$[\theta]_{222}$ SUV ^g	% α -helix SUV ^f
Gly-12	hg	0	11.5 \pm 1.4	-17 760	52	-24 798	73
Gly-9	hg/ac	0	11.0 \pm 0.9	-18 335	54	-20 091	59
Gly-7	ac	0	12.3 \pm 1.3	-16 763	49	-22 676	67
Ala-12	hg	0.32 \pm 0.14	11.7 \pm 0.9	-26 071	77	-25 144	74
Ala-9	hg/ac	0.57 \pm 0.18	11.3 \pm 1.1	-27 573	82	-25 869	77
Ala-7	ac	0.40 \pm 0.19	11.8 \pm 1.0	-24 065	70	-26 556	78
Val-12	hg	0.99 \pm 0.17	11.3 \pm 2.1	-25 037	73	-26 909	79
Val-9	hg/ac	0.93 \pm 0.11	11.5 \pm 1.3	-23 437	68	-26 935	79
Val-7	ac	1.12 \pm 0.17	12.0 \pm 0.8	-23 441	69	-25 609	76
Ile-12	hg	1.60 \pm 0.16	11.3 \pm 1.1	-25 633	75	-24 085	72
Ile-9	hg/ac	1.60 \pm 0.17	12.0 \pm 1.3	-23 941	70	-25 873	76
Ile-7	ac	1.67 \pm 0.17	12.2 \pm 1.3	-24 527	72	-24 352	71
Leu-12	hg	1.56 \pm 0.17	12.0 \pm 2.4	-25 906	76	-25 633	75
Leu-9	hg/ac	1.50 \pm 0.16	11.7 \pm 0.9	-26 071	77	-25 144	74
Leu-7	ac	1.77 \pm 0.12	11.7 \pm 0.9	-26 071	77	-25 144	74

^a The guest residues were substituted into the peptide host (helix5) which has the amino acid² sequence Ac-NELKKKLELCKAK-WLEAKKKLEALK-NH₂. The cysteine residues at position 10 were spin-labeled with MTSSL. ^b Abbreviations: hg, headgroup; ac, acyl chain.

^c The $\Delta\Delta G_{tr}$ values (relative to Gly) for membrane–water transfer correspond to the nonelectrostatic contributions of the amino acid side chains to the standard-state differences in Gibbs transfer free energies at 25 °C. ^d The distances from nitroxide groups substituted at position 10 in the peptide variants to the phosphate groups in the phospholipid bilayers. ^e $[\theta]_{222}$ (deg cm² dmol⁻¹) at 25 °C, 5 mM potassium phosphate buffer, pH 7.0, 50 mM KCl. ^f The % α -helix values were determined by TFE titration (see Materials and Methods). ^g $[\theta]_{222}$ (deg cm² dmol⁻¹) at 25 °C, 5 mM potassium phosphate buffer, pH 7.0, 50 mM KCl, 15 mM of 15 mol % POPG/POPC in SUVs.

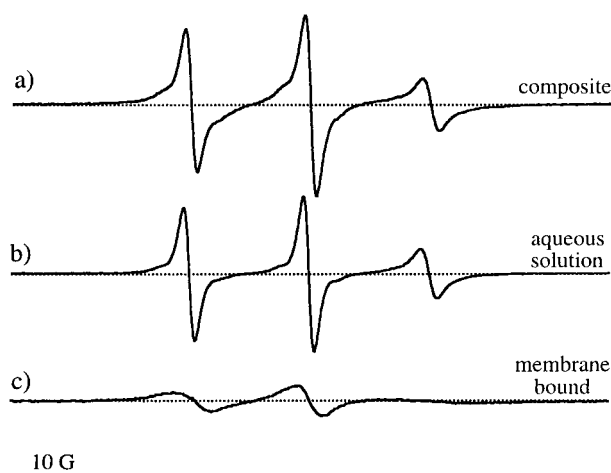


FIGURE 2: Continuous-wave EPR spectra for the host peptide helix5 in 5 mM MOPS buffer (pH 7.0, 50 mM NH₄OAc) at 25 \pm 1 °C. Helix5 has Leu, Leu, and Ala residues at positions 7, 9, and 12, respectively. (a) EPR spectrum of helix5 in the presence of 50 mM LUVs containing 7.0 mol % POPG/POPC. The total peptide concentration is 116 μ M. The spectrum has two components: a sharp component corresponding to the peptide fraction free in aqueous solution and a broad component corresponding to the peptide bound to LUVs. (b) Fast-motional EPR spectrum of helix5 in aqueous solution in the absence of LUVs. The peptide concentration is 89 μ M. After subtracting the sharp solution spectrum of helix5 (b) from the two-component spectrum (a), the resulting broad component (c) corresponds to the bilayer-bound fraction of peptide. The concentrations of peptide bound to bilayers and free in solution were determined to be 56 and 60 μ M, respectively, for the sample shown in (a).

binding. The membrane affinities both in an α -helical context and as a function of bilayer depth are listed in Table 1.

Comparison of Membrane–Water Partitioning of Helix5 and Helix5b. To further study the bilayer-depth dependence of the membrane affinities, we synthesized and characterized the peptide helix5b. Helix5b's sequence is the same as helix5's except for Leu7Ala and Ala12Leu substitutions, so that the effective difference between the two peptides is switching the alanine and leucine residues at positions 7 and

12 in the sequences. When the peptides are bound to bilayers, position 7 (in the nonpolar face of the α -helix) is immersed in the acyl chain region of the bilayer, and position 12 (in the middle of the polar face of the α -helix) is immersed in the headgroup region (Figure 1b). CD experiments showed that helix5b has α -helix contents of 73 and 70% in aqueous solution and in SUVs, respectively, which are similar to those of helix5. EPR spectral subtraction was used to determine the partitioning ratios (P_b/P_f) of helix5 and helix5b (25 °C, 5 mM MOPS buffer, pH 7.0, 50 mM NH₄OAc, 50 mM of 7 mol % POPG/POPC). The P_b/P_f values for helix5 and helix5b are 0.93 ± 0.08 and 0.84 ± 0.06 , respectively. From the partitioning data, the difference in transfer free energies of the two peptides ($\Delta\Delta G_{tr}$ for helix5b – helix5) was calculated to be 0.05 ± 0.14 kcal mol⁻¹. Therefore, the alanine–leucine interchange in the host peptide does not appear to significantly alter the water–membrane partitioning, further supporting the host–guest results that the $\Delta\Delta G_{tr}$ values are independent of immersion depth.

DISCUSSION

The purpose of this work was to experimentally determine the membrane affinities of the aliphatic amino acid side chains as a function of bilayer depth in an α -helical context. Table 1 lists the $\Delta\Delta G_{tr}$ values (relative to Gly) for the aliphatic guest residues which were substituted at guest sites located in the acyl chain region, the interface between the acyl chain and headgroup regions, and the headgroup region of the bilayers in the membrane-bound states. Due to nonideal behavior of the peptide host (less than 100% α -helical structure), exact quantitative interpretations of the $\Delta\Delta G_{tr}$ values in terms of an ideal, 100% α -helical reference state may not be easy. However, two semiquantitative interpretations of the data can be made. First, the $\Delta\Delta G_{tr}$ values for the aliphatic side chains do not vary significantly as a function of bilayer depth. Second, the $\Delta\Delta G_{tr}$ values for the aliphatic side chains in an α -helical context are reduced to approximately two-thirds of $\Delta\Delta G_{tr}$ values obtained from octanol–water transfer of *N*-acetyl-amino acid amides

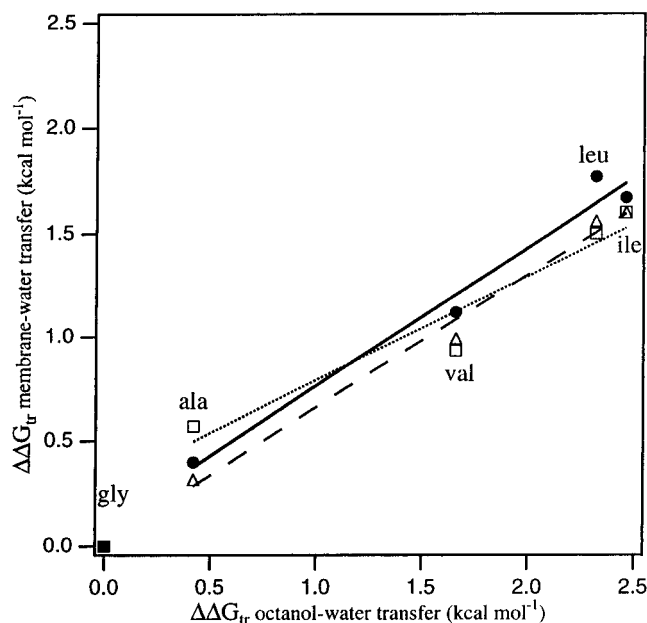


FIGURE 3: Differences in membrane–water transfer free energies ($\Delta\Delta G_{tr}$ relative to Gly) in an α -helical context plotted against differences in octanol–water transfer free energies (35, 56). The data shown include values determined for aliphatic guest residues substituted at positions 7 (●), 9 (□), and 12 (△) in the sequence of the host peptide, helix5. The experimental errors have been omitted from the figure for display purposes but are included in Table 1. The three lines represent linear least-squares fits to the data for Ala, Val, Ile, and Leu: position 7 (solid line, $m = 0.67 \pm 0.15$, $R = 0.988$), position 9 (dotted line, $m = 0.50 \pm 0.20$, $R = 0.964$), and position 12 (dashed line, $m = 0.64 \pm 0.10$, $R = 0.994$).

(Figure 3) and $\Delta\Delta G_{tr}$ values obtained from bilayer–water transfer in an extended/unordered peptide host (Figure 4).

The water–membrane partitioning of a peptide is determined by a complex combination of thermodynamic forces. The total change in standard-state Gibbs free energy upon transfer of a peptide from aqueous solution into bilayers (ΔG_{tot}) can be expressed as the sum of various free energy components (29):

$$\Delta G_{tot} = \Delta G_{hyd} + \Delta G_{el} + \Delta G_{lip} + \Delta G_{imm} + \Delta G_{con} + \Delta G_{H-bond} + \Delta G_{vdw} \quad (6)$$

The free energy components account for the hydrophobic effect (ΔG_{hyd}), electrostatic interactions (ΔG_{el}), lipid perturbations upon peptide insertion into bilayers (ΔG_{lip}), peptide immobilization in bilayers (ΔG_{imm}), peptide conformational changes (ΔG_{con}), hydrogen bonding (ΔG_{H-bond}), and van der Waals dispersion interactions (ΔG_{vdw}). In principle, each of the aforementioned thermodynamic forces may also contribute to the difference in Gibbs transfer free energies ($\Delta\Delta G_{tot}$) for two peptides differing only by one amino acid substitution at a guest site as follows:

$$\Delta\Delta G_{tot} = \Delta\Delta G_{hyd} + \Delta\Delta G_{el} + \Delta\Delta G_{lip} + \Delta\Delta G_{imm} + \Delta\Delta G_{con} + \Delta\Delta G_{H-bond} + \Delta\Delta G_{vdw} \quad (7)$$

The $\Delta\Delta G$ terms in eq 7 correspond to the energetic costs of side chain substitution between two peptides which undergo phase transfers, whereas the ΔG terms in eq 6 correspond to the energetic costs for the phase transfer of a single peptide. The aim of the present work was to determine the

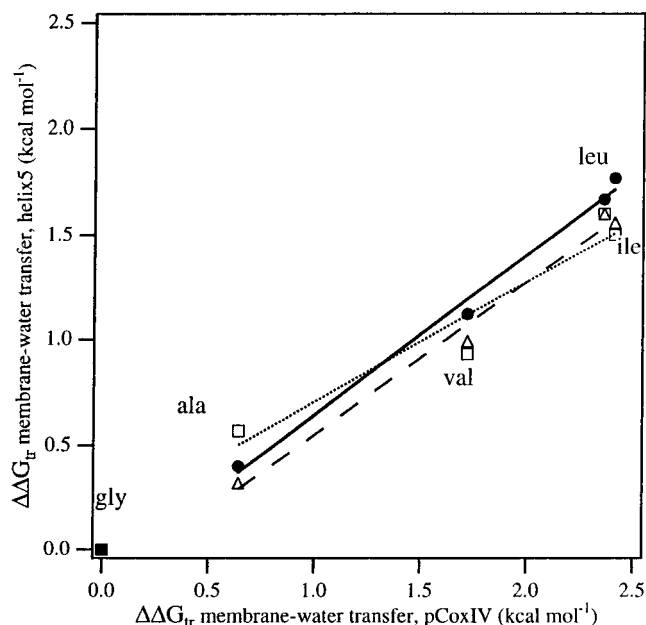


FIGURE 4: Differences in membrane–water transfer free energies ($\Delta\Delta G_{tr}$ relative to Gly) in an α -helical context plotted against differences in membrane–water transfer free energies in an extended/unordered context (31). The data shown include values determined for aliphatic guest residues substituted at positions 7 (●), 9 (□), and 12 (△) in the sequence of the host peptide, helix5. The three lines represent linear least-squares fits to the data for Ala, Val, Ile, and Leu: position 7 (solid line, $m = 0.76 \pm 0.10$, $R = 0.996$), position 9 (dotted line, $m = 0.57 \pm 0.23$, $R = 0.964$), and position 12 (dashed line, $m = 0.73 \pm 0.11$, $R = 0.994$).

$\Delta\Delta G_{tr}$ values ($\Delta\Delta G_{tr} = \Delta\Delta G_{tot} - \Delta\Delta G_{el}$) of the aliphatic side chains in the context of an α -helical peptide host which does not undergo structural changes due to the guest substitutions. The $\Delta\Delta G_{tr}$ values could then represent the intrinsic membrane affinities of the side chains independent of the secondary structural propensities of the side chains. For peptides which do not undergo structural changes due to guest substitutions, the $\Delta\Delta G_{tr}$ values would be expected to be independent of contributions from electrostatic interactions, peptide immobilization, peptide conformational changes, and hydrogen bonding (for the aliphatic side chains). Moreover, it is unlikely that the substitution of 1 amino acid residue in the context of a 25-residue host would result in a significant change in the lipid perturbations unless the amino acid substitution also caused peptide structural changes. Before interpreting the thermodynamic significance of the $\Delta\Delta G_{tr}$ values determined in this work, it is necessary to consider the structures of the peptides as a function of amino acid guest substitutions.

The peptide variants with Gly residues as guests have aqueous α -helix contents of approximately 52% and bilayer-bound α -helix contents which range from 59 to 73%, whereas the peptides with Ala, Val, Ile, and Leu residues as guests have α -helix contents of approximately 75% both in aqueous solution and in membranes. A quantitative comparison of the $\Delta\Delta G_{tr}$ values for the Gly variants with the $\Delta\Delta G_{tr}$ values for the Ala, Val, Ile, and Leu variants would be expected to be confounded by the significant structural differences between the Gly variants and the other aliphatic variants. Quantitative comparison of the $\Delta\Delta G_{tr}$ values for the peptides with Ala, Val, Ile, and Leu as guests should be more straightforward since they have α -helix contents of ap-

proximately 75% both in aqueous solution and in bilayers. The rank order of aqueous α -helix propensities using other peptide hosts is Val < Ile < Leu < Ala (42–44). One explanation for the relative guest tolerance of helix5 in comparison to other hosts is that the α -helical structure of helix5 may be significantly stabilized by oppositely charged residues at $i, i + 3$ and $i, i + 4$ positions which can allow the formation of 11 ion pairs or salt bridges (33).

Bilayer-Depth Dependence of the Membrane Affinities. The $\Delta\Delta G_{tr}$ values determined in this study do not significantly vary as a function of the bilayer depth of the guest site (Table 1). Comparison of the bilayer binding of helix5 and helix5b further supports that the contributions of Ala and Leu residues to the binding of α -helical peptides to bilayers is independent of the bilayer depth of the residues. The invariance of the $\Delta\Delta G_{tr}$ values with respect to the bilayer depth of the guest sites is consistent with the hydrophobic effect being the dominant factor in determining the bilayer binding of peptides. The salient feature is that the nonpolar surface area of the guest residues is removed from bulk water. However, the $\Delta\Delta G_{tr}$ values of the polar and charged side chains may vary as a function of bilayer depth. Those $\Delta\Delta G_{tr}$ values have not yet been determined as a function of bilayer depth.

Studies on apolipoprotein mimetics show that an increase in the hydrophobicity of amino acid residues in the nonpolar face of amphipathic α -helices increases the lipid affinities of the peptides (46–48). The independence of the membrane affinities of the aliphatic amino acid side chains demonstrated in the present study shows that nonpolar residues located in the polar face of amphipathic α -helices also can contribute significantly to the bilayer binding of amphipathic α -helices as long as they are buried in a bilayer. For amphipathic helices in proteins, the residue hydrophobicity of the polar face may be a determining factor for membrane insertion vs coiled-coil formation. Membrane insertion of amphipathic α -helical regions with a large number of hydrophobic residues in the polar face may be favored over coiled-coil formation since the hydrophobic residues in the polar face would not be removed from an aqueous environment in the formation of coiled-coils but would in membrane binding. For example, a peptide from the heptad repeat region of the human immunodeficiency virus (HIV) gp41 has four Leu, one Val, one Trp, one Tyr, and four Ala residues in its polar face and nonpolar–polar interface (49). In the presence of an antiparallel buttressing peptide, the gp41 heptad repeat peptide forms a trimeric coiled-coil in aqueous solution (50, 51). However, the heptad repeat peptide selectively inserts into membranes when the peptides are introduced into aqueous lipid vesicle suspensions (52).

Structural Context Dependence of the Membrane Affinities. The $\Delta\Delta G_{tr}$ values determined in an α -helical context are reduced to approximately two-thirds of $\Delta\Delta G_{tr}$ values determined in other studies for the octanol–water and bilayer–water partitioning of guest amino acid side chains which are fully exposed to solvent in the aqueous states (31, 34, 35). The $\Delta\Delta G_{tr}$ values for bilayer–water transfer in the α -helical context correlate with the $\Delta\Delta G_{tr}$ values for octanol–water transfer (34, 35) with slopes of 0.67 ± 0.15 , 0.50 ± 0.20 , and 0.64 ± 0.10 for the peptide variants with guests at positions 7, 9, and 12, respectively (Figure 3). Figure 4 shows the bilayer–water $\Delta\Delta G_{tr}$ values in the α -helical context

plotted against membrane–water $\Delta\Delta G_{tr}$ values determined in an extended/unordered context (31). Thorgeirsson et al. (31) used a peptide variant of the presequence of yeast cytochrome *c* oxidase subunit IV (pCoxIV) for a host–guest study, determining the membrane affinities of 14 uncharged amino acid side chains. The amino acid² sequence of the peptide host was ^+H_3N -MLSCRQXIRFFKPATRTLSSSR-YLL-COO[−], where X is the guest site in the peptide. The pCoxIV peptide host has an extended/unordered conformation in aqueous solution and when bound to bilayers, and the pCoxIV peptide host binds to bilayers parallel to the bilayer surface with the peptide backbone located in the headgroup region and the guest site (X) located in the acyl chain region of the bilayer (31). Figure 4 shows that the bilayer–water $\Delta\Delta G_{tr}$ values determined in this study in an α -helical context correlate with those determined in an extended/unordered context with slopes of 0.76 ± 0.09 , 0.57 ± 0.23 , and 0.73 ± 0.11 for the peptide variants with guests at positions 7, 9, and 12, respectively. The significant reduction in the membrane–water $\Delta\Delta G_{tr}$ values in the α -helical context in comparison to the extended/unordered context shows that the structural context of an aliphatic guest residue will in part determine the membrane affinity of a guest residue.

The most probable explanation for the reduction in $\Delta\Delta G_{tr}$ values in an α -helical context is that the α -helical structure near the guest site reduces the solvent-accessible surface area of the guest side chain, thereby reducing its hydrophobicity. Richards and Richmond (53) have calculated that the side chain contact area³ for Ala, Val, Ile, and Leu in the host peptide Ala₄-X-Ala₄ in an α -helix is an average of 18% less than the side chain contact area in an extended chain. A greater reduction in the side chain contact area of guests may occur in the context of the host peptide helix5 since the guest residues in the helix5 α -helix neighbor residues with larger van der Waals areas than alanine side chains. Since the hydrophobic effect is a major determinant of the membrane–water partitioning of peptides (29, 31), any structural changes resulting in increased or decreased exposure of nonpolar side chains to bulk water in the aqueous state would be expected to alter the energetics of bilayer binding of a peptide due to differences in the hydrophobic contribution to bilayer binding.

The structural context dependence of the membrane affinities of the aliphatic amino acid side chains has several implications in the understanding, predicting, and designing of the membrane binding of peptides. The magnitudes of the membrane affinities of the aliphatic amino acid side chains are determined in part by the structural context of the peptide in which they are located. The aqueous and membrane-bound structures of peptides are, in turn, largely determined by their amino acid sequences (C.J.R., in preparation). Therefore, amino acid sequence determines the aqueous and bilayer-bound structures of peptides, and the structures of peptides in part determine the membrane affinities of individual amino acid residues and, as a result,

³ The *contact area* has been defined as the area of accessible van der Waals surface that can be in contact with the tip of a probe used to estimate surface areas (1). In contrast, the more conventional *accessible surface area* is the area mapped by the center of a probe (which is typically a water molecule modeled as a sphere with a radius of 1.4 Å).

entire peptides. To predict the bilayer–water partitioning of a given peptide, prediction of the peptide's structure will be necessary to estimate the membrane affinities of the peptide's constituent amino acid residues. In addition, peptide sequence and structure will also have to be considered when designing the bilayer binding of de novo-designed peptides since structural context is a determinant of the magnitudes of the membrane affinities of individual amino acid residues.

Comparison to Other Experimentally Determined Membrane Affinities. Several other studies report experimentally determined values for the membrane affinities of amino acid residues in non- α -helical peptide hosts (27, 31, 32). The rank order for the $\Delta\Delta G_{tr}$ values of the aliphatic residues determined using the extended/unordered pCoxIV host (31) is the same as that in the context of the α -helical peptide host: Gly < Ala < Val < Ile \approx Leu. Moreover, the $\Delta\Delta G_{tr}$ values of 14 uncharged amino acid side chains determined using the pCoxIV host correlate well with $\Delta\Delta G_{tr}$ values for octanol–water partitioning obtained for *N*-acetyl-amino acid amides with a slope of 1.04 (31). These values are consistent with the $\Delta\Delta G_{tr}$ values for the guest residues arising in both cases due to the hydrophobic effect (removal of nonpolar surface area from bulk water). The slope of a plot of the $\Delta\Delta G_{tr}$ values obtained using the pCoxIV host vs $\Delta\Delta G_{tr}$ values for octanol–water partitioning obtained using the host Ac-Trp-Leu-X-Leu-Leu (54) has a value of 1.30. The larger slope is due to the smaller magnitudes of the $\Delta\Delta G_{tr}$ values for octanol–water transfer determined using the pentapeptide host in comparison to those determined using *N*-acetyl-amino acid amides. In the pentapeptide host, leucine residues flank the guest site and reduce the solvent accessibility of the guest site (32). It is possible that similar occlusion effects occur in the 25-residue pCox peptide which has the sequence -Arg-Gln-X-Ile-Arg- flanking the guest site (X). However, electrostatic repulsions between the *i*, *i* + 4 Arg residues would tend to maximize the distance between those residues, and it is known that the peptide adopts extended conformations in aqueous solution and in bilayers (31).

White and co-workers also report experimentally determined values for the membrane affinities of individual amino acid residues (27, 32). The first study used the peptide host Ala-X-Ala-*O*-*tert*-butyl to determine the membrane affinities of Gly, Ala, Leu, Phe, and Trp side chains (27). Neutron diffraction studies showed that the most hydrophobic peptide studied was primarily located in the headgroup region of DOPC bilayers. The membrane–water $\Delta\Delta G_{tr}$ values obtained using the tripeptide host increase in the order Gly < Ala < Leu < Phe < Trp but are approximately only half as large as the membrane–water $\Delta\Delta G_{tr}$ values obtained with the pCoxIV host (31). The apparent reduction in $\Delta\Delta G_{tr}$ values obtained using the tripeptide host is consistent with incomplete burial of the guest residues in the bilayer (27, 55).

Wimley and White (32) used the pentapeptide host Ac-Trp-Leu-X-Leu-Leu to experimentally determine the water–membrane $\Delta\Delta G_{tr}$ values for all 20 naturally occurring amino acid residues. Under certain experimental conditions, the pentapeptide host lacks secondary structure and is expected to bind to membranes in the headgroup region based on experimental measurements and energetic considerations (32). The rank order for the transfer free energies of the aliphatic residues in the pentapeptide host (Ala < Val \approx

Gly < Ile < Leu) differs from that in this work and is inconsistent with a rank order expected for predominantly hydrophobic contributions to membrane binding (Gly < Ala < Val < Ile \approx Leu). Moreover, a plot of the bilayer–water $\Delta\Delta G_{tr}$ values vs octanol–water $\Delta\Delta G_{tr}$ values for all of the uncharged residues using the pentapeptide host for both transfer studies (32, 54) shows a correlation with a slope of 0.728. Comparison of the $\Delta\Delta G_{tr}$ values for only alanine and leucine gives a slope of approximately one-half (32). There are at least two possible explanations for the apparent reduction in water–membrane $\Delta\Delta G_{tr}$ values for the guests in the pentapeptide host in comparison to octanol–water $\Delta\Delta G_{tr}$ values. First, guest-specific changes in peptide secondary structure, membrane binding, and/or lipid perturbations due to amino acid substitutions in the context of the pentapeptide host could lead to energetic terms other than water–membrane partitioning contributing to the $\Delta\Delta G_{tr}$ values (32). Second, the hydrophobicities of the polar residues in the pentapeptide host may be reduced when located in the headgroup region of the bilayer due to polarity gradients in bilayers. The second explanation does not account for the observed rank order of the membrane affinities of the aliphatic amino acid residues (Ala < Val \approx Gly < Ile < Leu). However, the second explanation can be tested directly by experimental studies similar to those reported in this work using the complete set of amino acid residues as guests.

While the results from the present work and others (27, 31, 32) have some inconsistencies, several observations are apparent when considering all of the results together. First, the $\Delta\Delta G_{tr}$ values for bilayer–water transfer correlate well with $\Delta\Delta G_{tr}$ values for octanol–water transfer when the peptide hosts do not undergo significant structural changes due to guest substitutions. This observation is consistent with the hydrophobic effect playing a key role in the bilayer binding of amino acid residues in the context of peptide hosts. Second, the slopes of $\Delta\Delta G_{tr}$ values for bilayer–water transfer vs $\Delta\Delta G_{tr}$ values for octanol–water transfer may depend on factors which modulate the hydrophobicities of amino acid side chains. For example, the membrane affinity of a given amino acid side chain may vary depending on structural context. More exact relationships between peptide structure and bilayer–water partitioning may emerge as more experimental studies are performed to determine the membrane affinities of amino acid side chains using other peptide hosts.

CONCLUSIONS

In conclusion, the membrane affinities of the aliphatic amino acid residues have been determined as a function of bilayer depth in the context of an α -helical peptide host. The membrane affinities of the aliphatic side chains do not vary as a function of the depth of the guest site in the bilayer. The membrane affinities determined in the context of an α -helical peptide host are approximately two-thirds of membrane affinities previously determined in the context of an extended/unordered peptide host (31). Both results are consistent with the hydrophobic effect playing a key role in the binding of peptides to bilayers. With respect to the aliphatic amino acid side chains, hydrophobicity is apparently modulated by the solvent accessibility of guest residues but not by the depth of the guest residues in bilayers. The invariance of the membrane affinities of the aliphatic side

chains with respect to bilayer depth may play a role in structural differentiation between coil-coil formation and membrane binding by amphipathic α -helices in peptides and proteins.

ACKNOWLEDGMENT

We thank Zev Gartner for help with peptide purification and spin-labeling. We thank Dr. David S. King and the Howard Hughes Medical Institute for mass spectrometry and the use of their CD spectropolarimeter. We also thank Dr. Susan Marqusee for the use of her CD spectropolarimeter. We thank Dr. Christian Altenbach for giving us the protocol for preparation of Ni-EDDA.

REFERENCES

- Richards, F. M. (1977) *Annu. Rev. Biophys. Bioeng.* 6, 151–176.
- Engelman, D. M. (1996) *Science* 274, 1850–1851.
- Engelman, D. M., and Steitz, T. A. (1981) *Cell* 23, 411–422.
- von Heijne, G. (1995) *Bioessays* 17, 25–30.
- Bark, I. C., and Wilson, M. C. (1994) *Proc. Natl. Acad. Sci. U.S.A.* 91, 4621–4624.
- Rothman, J. E. (1996) *Protein Sci.* 5, 185–194.
- Hernandez, L. D., Hoffman, L. R., Wolfsberg, T. G., and White, J. E. (1996) *Ann. Rev. Cell Dev. Biol.* 12, 627–661.
- Hughson, F. M. (1997) *Curr. Biol.* 7, R565–R569.
- Stegmann, T. (1994) *Curr. Biol.* 4, 551–554.
- Myles, D. G., and Primakoff, P. (1997) *Biol. Reprod.* 56, 320–327.
- Wassarman, P. M. (1995) *Curr. Opin. Cell Biol.* 7, 658–664.
- Ganz, T., and Lehrer, R. I. (1994) *Curr. Opin. Immunol.* 6, 584–589.
- Jack, R. W., Tagg, J. R., and Ray, B. (1995) *Microbiol. Rev.* 59, 171–200.
- Nicolas, P., Mor, A. (1995) *Annu. Rev. Microbiol.* 49, 277–304.
- Lesieur, C., et al. (1997) *Mol. Membr. Biol.* 14, 45–64.
- Martoglio, B., Hofmann, M. W., Brunner, J., and Dobberstein, B. (1995) *Cell* 81, 207–214.
- Randall, L. L., Hardy, S. J., and Thom, J. R. (1987) *Annu. Rev. Microbiol.* 41, 507–541.
- Pfanner, N., and Neupert, W. (1990) *Annu. Rev. Biochem.* 59, 331–353.
- von Heijne, G. (1988) *Biochim. Biophys. Acta* 947, 307–333.
- Tanford, C. (1980) *The Hydrophobic Effect: Formation of Micelles and Biological Membranes*, 2nd ed., John Wiley & Sons, New York.
- Nakai, K., Kidera, A., and Kanehisa, M. (1988) *Protein Eng.* 2, 93–100.
- Marqusee, J. A., and Dill, K. A. (1986) *J. Chem. Phys.* 85, 434–444.
- Seelig, A., and Seelig, J. (1977) *Biochemistry* 16, 45–50.
- Wiener, M. C., and White, S. H. (1992) *Biophys. J.* 61, 437–447.
- Flewellling, R. F., and Hubbell, W. L. (1986) *Biophys. J.* 49, 541–552.
- Ben-Tal, N., Ben, S. A., Nicholls, A., and Honig, B. (1996) *Biophys. J.* 70, 1803–1812.
- Jacobs, R. E., and White, S. H. (1989) *Biochemistry* 28, 3421–3437.
- Jähnig, F. (1983) *Proc. Natl. Acad. Sci. U.S.A.* 80, 3691–3695.
- Russell, C. J., Thorgeirsson, T. E., and Shin, Y. K. (1996) *Biochemistry* 35, 9526–9532.
- Jain, M. K., Rogers, J., Simpson, L., and Gierasch, L. M. (1985) *Biochim. Biophys. Acta* 816, 153–162.
- Thorgeirsson, T. E., Russell, C. J., King, D. S., and Shin, Y.-K. (1996) *Biochemistry* 35, 1803–1809.
- Wimley, W. C., and White, S. H. (1996) *Nat. Struct. Biol.* 3, 842–848.
- Russell, C. J., King, D. S., Thorgeirsson, T. E., and Shin, Y.-K. (1998) *Protein Eng.* 11, 539–547.
- Eisenberg, D., and McLachlan, A. D. (1991) *Biochim. Biophys. Acta* 1061, 297–303.
- Fauchere, J.-L., and Pliska, V. (1983) *Eur. J. Med. Chem.-Chim. Ther.* 18, 369–375.
- King, D. S., Fields, C. G., and Fields, G. B. (1990) *Int. J. Pept. Protein Res.* 36, 255–266.
- Edelhoch, H. (1967) *Biochemistry* 6, 1948–1954.
- Chakrabarty, A., Kortemme, T., Padmanabhan, S., and Baldwin, R. L. (1993) *Biochemistry* 32, 5560–5565.
- Altenbach, C., Greenhalgh, D. A., Khorana, H. G., and Hubbell, W. L. (1994) *Proc. Natl. Acad. Sci. U.S.A.* 91, 1667–1671.
- Kauzmann, W. (1959) *Adv. Protein Chem.* 14, 1–57.
- Thorgeirsson, T. E., Yu, Y. G., and Shin, Y. K. (1995) *Biochemistry* 34, 5518–5522.
- Baldwin, R. L. (1995) *Biophys. Chem.* 55, 127–135.
- Muñoz, V., and Serrano, L. (1995) *J. Mol. Biol.* 245, 275–296.
- O'Neil, K. T., and DeGrado, W. F. (1990) *Science* 250, 646–651.
- Segrest, J. P., Jackson, R. L., Morrisett, J. D., and Gotto, A. J. (1974) *FEBS Lett.* 38, 247–258.
- Anantharamaiah, G. M., et al. (1988) *J. Lipid Res.* 29, 309–318.
- Fukushima, D., Yokoyama, S., Kroon, D. J., Kezdy, F. J., and Kaiser, E. T. (1980) *J. Biol. Chem.* 255, 10651–10657.
- Kanellis, P., et al. (1980) *J. Biol. Chem.* 255, 11464–11472.
- Rabenstein, M., and Shin, Y. K. (1995) *Biochemistry* 34, 13390–13397.
- Chan, D. C., Fass, D., Berger, J. M., and Kim, P. S. (1997) *Cell* 89, 263–273.
- Weissenhorn, W., Dessen, A., Harrison, S. C., Skehel, J. J., and Wiley, D. C. (1997) *Nature* 387, 426–430.
- Rabenstein, M. D. (1996) Ph.D. Thesis, University of California, Berkeley.
- Richards, F. M., and Richmond, T. (1977) *Ciba Found. Symp.* 1977, 23–45.
- Wimley, W. C., Creamer, T. P., and White, S. H. (1996) *Biochemistry* 35, 5109–5124.
- White, S. H., and Wimley, W. C. (1994) *Curr. Opin. Struct. Biol.* 4, 79–86.
- Eisenberg, D. M., McLachlan, A. (1986) *Nature* 319, 199–203.

BI981179H